
Fidelity of base-pair recognition by a 3′–5′ polymerase: mechanism of the *Saccharomyces cerevisiae* tRNA^{His} guanylyltransferase

KRISHNA J. PATEL, PAUL YOURIK, and JANE E. JACKMAN

Department of Chemistry and Biochemistry, Center for RNA Biology, The Ohio State University, Columbus, Ohio 43210, USA

ABSTRACT

The tRNA^{His} guanylyltransferase (Thg1) was originally discovered in *Saccharomyces cerevisiae* where it catalyzes 3′–5′ addition of a single nontemplated guanosine (G₋₁) to the 5′ end of tRNA^{His}. In addition to this activity, *S. cerevisiae* Thg1 (SceThg1) also catalyzes 3′–5′ polymerization of Watson–Crick (WC) base pairs, utilizing nucleotides in the 3′-end of a tRNA as the template for addition. Subsequent investigation revealed an entire class of enzymes related to Thg1, called Thg1-like proteins (TLPs). TLPs are found in all three domains of life and preferentially catalyze 3′–5′ polymerase activity, utilizing this unusual activity to repair tRNA, among other functions. Although both Thg1 and TLPs utilize the same chemical mechanism, the molecular basis for differences between WC-dependent (catalyzed by Thg1 and TLPs) and non-WC-dependent (catalyzed exclusively by Thg1) reactions has not been fully elucidated. Here we investigate the mechanism of base-pair recognition by 3′–5′ polymerases using transient kinetic assays, and identify Thg1-specific residues that play a role in base-pair discrimination. We reveal that, regardless of the identity of the opposing nucleotide in the RNA “template,” addition of a non-WC G₋₁ residue is driven by a unique kinetic preference for GTP. However, a secondary preference for forming WC base pairs is evident for all possible templating residues. Similar to canonical 5′–3′ polymerases, nucleotide addition by SceThg1 is driven by the maximal rate rather than by NTP substrate affinity. Together, these data provide new insights into the mechanism of base-pair recognition by 3′–5′ polymerases.

Keywords: RNA polymerase; single-turnover kinetics; RNA processing; Thg1; TLP

INTRODUCTION

DNA and RNA polymerases maintain the integrity of transmission and expression of genetic information in all domains of life. Canonical polymerases catalyze addition of nucleotides in the 5′–3′ direction using a two-metal ion catalytic mechanism (Joyce and Steitz 1995; Steitz 1998, 1999). This conserved reaction involves nucleophilic attack of the 3′-OH from a growing polynucleotide chain on the α-phosphate of an incoming nucleoside triphosphate (NTP), resulting in phosphodiester bond formation and pyrophosphate release (Fig. 1A). Similar chemistry could be used to polymerize nucleotides in the 3′–5′ direction with the same functional groups. For this reaction, the 3′-OH of an incoming NTP would attack the 5′ triphosphorylated end of the growing polynucleotide chain to create the same phosphodiester linkage as for 5′–3′ addition (Fig. 1A). Enzymes of the tRNA^{His} guanylyltransferase (Thg1)/Thg1-like protein (TLP) superfamily are so far the only

known enzymes that utilize this 3′–5′ RNA polymerase chemistry (Gu et al. 2003; Jackman et al. 2012; Chen et al. 2019).

In eukaryotes, as initially demonstrated in *Saccharomyces cerevisiae*, Thg1 utilizes the 3′–5′ nucleotide addition reaction to catalyze the essential addition of a single guanosine (G₋₁) nucleotide to the 5′-end of tRNA^{His} (Fig. 1B; Gu et al. 2003, 2005). The G₋₁ addition reaction catalyzed by SceThg1 plays a critical role in maintaining the fidelity of protein synthesis because G₋₁ is required for recognition of tRNA^{His} by histidyl-tRNA synthetase (HisRS) (Rudinger et al. 1994, 1997; Nameki et al. 1995; Rosen et al. 2006). SceThg1 incorporates GTP opposite a universally conserved A₇₃ nucleotide to form a non-WC G₋₁:A₇₃ base pair (Fig. 1B). Therefore, it was surprising when in vitro studies revealed the ability of SceThg1 to catalyze an alternative activity that could utilize the 3′-end of an

© 2021 Patel et al. This article is distributed exclusively by the RNA Society for the first 12 months after the full-issue publication date (see <http://majournal.cshlp.org/site/misc/terms.xhtml>). After 12 months, it is available under a Creative Commons License (Attribution-NonCommercial 4.0 International), as described at <http://creativecommons.org/licenses/by-nc/4.0/>.

Corresponding author: jackman.14@osu.edu

Article is online at <http://www.majournal.org/cgi/doi/10.1261/rna.078686.121>.

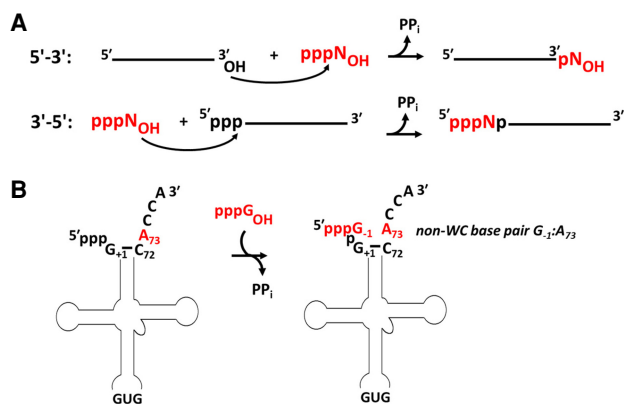


FIGURE 1. 3'-5' polymerase activities catalyzed by Thg1-family enzymes. (A) Comparison of the chemistry of nucleotidyl transfer during 5'-3' versus 3'-5' polymerase reactions. In each case, a hydroxyl nucleophile attacks a nucleotide 5'-triphosphate, releasing PP_i as a leaving group and resulting in the formation of a phosphodiester bond. However, the orientation of the hydroxyl and triphosphate functional groups are reversed between the two reactions. Arrows indicate the location of the initial nucleophilic attack on each triphosphate. (B) Schematic of the use of 3'-5' polymerase chemistry to add G₋₁ to wild-type tRNA^{His} containing the A₇₃ discriminator nucleotide. The reaction shown is the *in vitro* reaction that occurs with 5'-triphosphorylated tRNA^{His} transcripts, which were used for kinetic characterization in this work.

engineered tRNA as the template for 3'-5' polymerization of multiple WC base pairs (Jackman and Phizicky 2006b). Subsequent studies suggested that, in fact, the 3'-5' polymerase activity is the ancestral activity of this enzyme family, and that the non-WC dependent G₋₁ addition reaction observed in yeast and other eukaryotes was likely acquired as a specialized trait during evolution of the eukaryotic enzymes (Abad et al. 2010; Rao et al. 2011; Long et al. 2016; Chen et al. 2019).

The ability to efficiently incorporate two distinct kinds of base pairs (WC and non-WC), depending on the identity of the RNA substrate, remains so far, an exclusive property of Thg1-type enzymes from eukaryotes (Jackman and Phizicky 2006b; Abad et al. 2010; Rao et al. 2011; Nakamura et al. 2018a). Yet questions remain about the molecular basis for the fidelity of base-pair selection by Thg1/TLP enzymes. Interest in these questions was further heightened by multiple crystal structures now available for members of this enzyme family, all demonstrating significant structural similarity between the active sites of Thg1/TLP 3'-5' polymerases and canonical WC-dependent 5'-3' DNA/RNA polymerases (Hyde et al. 2010, 2013; Nakamura et al. 2013; Kimura et al. 2016). Similar arrangement of the two metal ions and NTP binding sites, combined with the results of alterations to conserved active-site residues suggested that both 5'-3' and 3'-5' polymerases share the same two metal-ion mechanism for catalysis. Decades of structural and biochemical studies have probed mechanisms of base-pair selection by multi-

ple members of the canonical 5'-3' polymerase family (Kuchta et al. 1988; Johnson and Johnson 2001; Fiala and Suo 2004; Joyce and Benkovic 2004; Roettger et al. 2004; Brown et al. 2010), but the molecular principles that drive base-pair selection in the context of 3'-5' polymerases are only beginning to be understood. Several recent investigations of base-pair recognition, including a kinetic study with *C. albicans* Thg1 (see below) and biochemical studies with human Thg1 have underscored that there are biochemically distinct features associated with WC versus non-WC reactions (Nakamura et al. 2018b; Matlock et al. 2019).

Here we describe a comprehensive kinetic investigation into the mechanism of base-pair selection by 3'-5' polymerases using full-length tRNA^{His} substrates, and identification of protein residues that play a unique role in the discrimination between WC and non-WC base pairs by SceThg1. We show that the ability to add the non-WC base-paired G₋₁ is driven largely by a kinetic preference for GTP nucleotide substrates, and is a bona fide nontemplated reaction, occurring with high catalytic efficiency regardless of the identity of the tRNA N₇₃ discriminator nucleotide. In addition, investigation of variants of highly conserved residues that are shared by Thg1, but not by TLP members of the 3'-5' polymerase family, reveals three Thg1 residues that when altered impact non-WC GTP addition, but not WC-dependent 3'-5' addition, thus indicating distinct sites for recognition of the two types of base pairs. Through these studies we provide new insights into the mechanism of catalysis utilized by these unique reverse polymerases and suggest a conserved mechanism of base-pair fidelity as carried out by both 5'-3' and 3'-5' polymerase enzymes.

RESULTS

SceThg1 exhibits distinct preferences for GTP versus WC base-paired NTP additions

Because of the similarities between 5'-3' and 3'-5' polymerase chemistry (Fig. 1A), we sought to compare the fidelity of base-pair selection using a similar kinetic framework to that widely used for characterizing fidelity of 5'-3' polymerase enzymes. Specifically, measured rates of NTP incorporations with a series of substrates where the identity of the templating nucleotide base could be varied systematically. For its biological G₋₁ addition activity, SceThg1 uses a three step reaction involving first, 5'-end activation by ATP to add G₋₁ to the tRNA^{His} substrate, which is 5'-monophosphorylated due to the prior action of the 5'-end maturation enzyme Ribonuclease P, and thus 5'-adenylylated tRNA^{His} is the substrate for nucleotidyl transfer *in vivo* (Jahn and Pande 1991; Jackman and Phizicky 2006a; Smith and Jackman 2012). However, we previously developed single-turnover kinetic assays that enable

individual characterization of the three chemical steps (5'-adenylation, nucleotidyl transfer, 5'-pyrophosphate removal) that occur during G_{-1} addition. We used these assays to demonstrate that SceThg1 exhibits nucleotidyl transfer activity with its biological 5'-adenylated tRNA^{His} substrate with the same rate as it does with 5'-triphosphorylated tRNA^{His} (ppp-tRNA) that can be readily prepared by in vitro transcription (Smith and Jackman 2012). Importantly, ppp-tRNA is also the relevant substrate for multiple nucleotide 3'-5' polymerase reactions, which use the 5'-ppp end that results from the previous NTP addition as the substrate for attack by the incoming NTP, as diagrammed in Figure 1A (Jackman and Phizicky 2006b; Abad et al. 2011, 2014). For all of these reasons, we chose to use ppp-tRNA substrates for this work (as shown in Fig. 1B), and measured complete kinetic profiles for the nucleotidyl transfer step for comparison to the well-characterized 5'-3' polymerase enzymes.

Another kinetic study of NTP addition by Thg1 was recently reported, using a novel two-piece tRNA system where a shorter 5'-fragment and 3'-template RNA are annealed, allowing nucleotide addition products to be resolved by gel electrophoresis (Nakamura et al. 2018b). Although there are many important advantages to this assay, some significant limitations to this system were revealed by a comparison to the complete kinetic characterization with full-length tRNA performed here. Our results are also compared with those from the two-piece tRNA system (see below) to clearly identify points where the two types of approaches agree, and where there are differences that indicate features important for understanding activity with the physiologically relevant tRNA.

We determined rates of nucleotidyl transfer catalyzed by SceThg1 under single-turnover conditions (where $[SceThg1]/[tRNA] \geq 5$). Reactions were performed with γ -³²P-labeled *ppp-tRNA substrates and varied concentration of each NTP, with product formation measured by the amount of labeled pyrophosphate (PPi) that is released after NTP addition to the 5'-end of each tRNA (Fig. 2A). Reaction progress curves were fit to a single exponential equation (Equation 1) to generate the observed rate (k_{obs}) at each concentration of NTP (Fig. 2B), and these k_{obs} determined at each (NTP) were then fit to a hyperbolic equation (Equation 2) to determine the pseudo-first order maximal rate constant for NTP addition (k_{pol}) and apparent dissociation constant (K_D) for each base-paired combination tested in the reactions (Fig. 2C). Using this approach, kinetic parameters were determined for all 16 possible NTP:N₇₃ tRNA^{His} base-pair combinations (Table 1). From these measured parameters, the k_{pol}/K_D value, which corresponds to the overall catalytic efficiency of a given reaction and is thus the best parameter to compare reactions with different substrates, was calculated.

The absolutely conserved nature of the A₇₃ discriminator nucleotide in eukaryotic tRNA^{His} raised the possibility

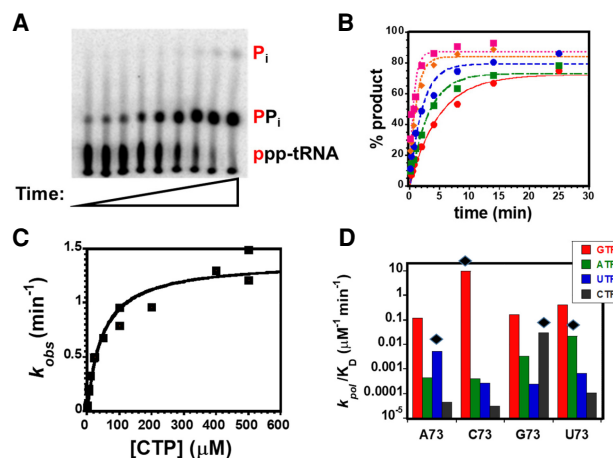


FIGURE 2. Single-turnover kinetic analysis of Thg1 3'-5' addition activity with tRNA substrates. (A) Representative time course of Thg1 nucleotidyl transfer activity. 5'-*ppp-tRNA^{His} (position of the labeled phosphate indicated in red) substrates are resolved from the PPi products of nucleotidyl transfer by thin-layer chromatography, as described in Materials and Methods. At longer times, some of the PPi is further hydrolyzed to Pi, and both products are quantified to measure % product formation as a function of time. (B) Measurement of single-turnover k_{obs} values for individual time courses was performed as described in Materials and Methods, with reaction progress curves fit to Equation 1 to yield k_{obs} for the indicated substrate and [NTP]. In this representative example, CTP addition to ppp-G₇₃tRNA^{His} was observed at 5 μ M (red), 10 μ M (green), 20 μ M (blue), 100 μ M (orange), and 500 μ M (pink) CTP. (C) Determination of maximal rate (k_{pol}) and apparent dissociation constant for NTP (K_D) from the plot of k_{obs} at each [CTP], as shown in B. Data shown are from three independent experiments plotted together and fit to Equation 2. (D) Catalytic efficiency (k_{pol}/K_D) measurements for nucleotidyl transfer reactions catalyzed by SceThg1 with all four N₇₃ tRNA^{His} templates and each NTP substrate, as indicated. For comparison, the tRNA substrates are presented with the physiological tRNA^{His} (A₇₃) substrate first, followed by results with the C₇₃ substrate that enables WC base-pairing with the physiologically relevant GTP nucleotide. The order shown for the NTP substrates also starts with GTP for the same reason (and shows results for the two purine NTPs followed by the two pyrimidines). Diamond symbols indicate the bar for the NTP that makes a WC base-pair with each N₇₃ substrate.

that selection of the GTP substrate might be due to recognition of some specific biochemical feature of the non-WC G-A base pair itself, particularly since a sheared G-A base pair is known to be stabilizing at the terminus of RNA duplexes (Chen et al. 2006). However, SceThg1 selects GTP with the highest catalytic efficiency regardless of the identity of the N₇₃ nucleotide (Fig. 2D red bars, Table 1). Moreover, the efficiencies of forming any of the three non-WC GTP:N₇₃ base pairs (G:A, G:G, or G:U) are nearly identical. These data eliminate an essential role for the conserved A₇₃ acting as a true "templating" nucleotide that enables selection of GTP over other possible nucleotides for G_{-1} addition in eukaryotes. Aside from the obvious preference for GTP during 3'-5' addition, a second trend was readily apparent. Apart from C₇₃-tRNA^{His}, the second-most efficiently incorporated NTP for any of the

TABLE 1. Kinetic parameters of NTP incorporation with N₇₃-tRNA^{His} variants catalyzed by SceThg1

NTP	k_{pol} (min ⁻¹)	K_D (μM)	k_{pol}/K_D (μM ⁻¹ min ⁻¹)	GTP preference ^a	WC preference ^b
Template A ₇₃ tRNA ^{His}					
GTP	2.84 ± 0.08	23 ± 2	1.2 × 10 ⁻¹	1	0.046
ATP	0.032 ± 0.001	70 ± 15	4.6 × 10 ⁻⁴	260	12
UTP	0.77 ± 0.07	140 ± 50	5.5 × 10 ⁻³	22	1
CTP	0.009 ± 0.001	200 ± 130	4.5 × 10 ⁻⁵	2700	120
Template C ₇₃ tRNA ^{His}					
GTP	≥10	≤1	≥10	1	1
ATP	0.065 ± 0.005	160 ± 40	4.1 × 10 ⁻⁴	24,000	24,000
UTP	0.14 ± 0.02	510 ± 160	2.7 × 10 ⁻⁴	37,000	37,000
CTP	0.10 ± 0.01	3000 ± 500	3.3 × 10 ⁻⁵	300,000	300,000
Template G ₇₃ tRNA ^{His}					
GTP	3.56 ± 0.39	22 ± 8	1.6 × 10 ⁻¹	1	0.18
ATP	0.16 ± 0.01	46 ± 13	3.5 × 10 ⁻³	47	9
UTP	0.11 ± 0.01	452 ± 170	2.4 × 10 ⁻⁴	670	120
CTP	1.38 ± 0.07	46 ± 9	3.0 × 10 ⁻²	5	1
Template U ₇₃ tRNA ^{His}					
GTP	4.88 ± 0.44	12 ± 4	4.1 × 10 ⁻¹	1	0.056
ATP	0.46 ± 0.03	20 ± 6	2.3 × 10 ⁻²	17	1
UTP	0.25 ± 0.02	362 ± 72	6.9 × 10 ⁻⁴	580	33
CTP	0.07 ± 0.008	628 ± 258	1.1 × 10 ⁻⁴	3600	210

^aCalculated as $(k_{pol}/K_D)_{GTP}/(k_{pol}/K_D)_{NTP}$ for the indicated NTP-tRNA combination.

^bCalculated as $(k_{pol}/K_D)_{WC}/(k_{pol}/K_D)_{non-WC}$ for the indicated NTP-tRNA combination.

other three N₇₃ template residues was the correct WC base-pairing NTP (Fig. 2D, bars marked with diamond symbols, Table 1).

Canonical 5′–3′ polymerase fidelity has been evaluated quantitatively by comparing k_{pol}/K_D values for different base-pair combinations (Kuchta et al. 1988; Joyce and Benkovic 2004; Roettger et al. 2004). In the case of SceThg1, to account for two distinct types of base-pairing reactions, we defined two separate fidelity parameters. One of these, the GTP preference (Table 1) corresponds to the ratio of k_{pol}/K_D for GTP incorporation compared to the k_{pol}/K_D for other NTP additions to a given substrate, with a higher value indicating that a base pair made with GTP is much more preferred than a base pair made with the tested NTP. The GTP preference exhibited by SceThg1 ranged from 5 to 300,000, indicating significant context dependence for the enzyme's preference for GTP over other possible NTP substrates. Not surprisingly, the strongest preferences for GTP over other possible NTPs (~10⁴–10⁵-fold) were observed in the context of the C₇₃ substrates where the inherent preference for GTP is also combined with the ability of this nucleotide to make a WC G₋₁:C₇₃ base pair (Table 1). The second fidelity parameter we defined is the WC preference, which is the ratio of the WC k_{pol}/K_D compared to the k_{pol}/K_D for other non-WC base-pair combinations, as has been classically

associated with other polymerases. Here, excluding comparisons with reactions involving GTP (and therefore subject to the inherent GTP preference), the preference of SceThg1 for forming WC base pairs over other non-WC combinations is modest, but readily measurable in all cases, varying from ~10–200-fold (Table 1).

Some similarities were observed between these trends and those observed in the previous analysis with the two-piece tRNA system (Nakamura et al. 2018b). However, there are two key differences that affect the interpretations from these two studies. First, overall rates measured with the two-piece substrates were substantially lower by ~2 orders of magnitude than those measured here with the full-length tRNA. Thus, activity with most non-WC base-pairing combinations (ATP or CTP with A₇₃, ATP, UTP or CTP with C₇₃, ATP or UTP with G₇₃, and UTP or CTP with U₇₃) could not be detected with the two-piece tRNA. Therefore, relative preferences for all different base-pair combinations could not be determined as they were here with the full-length tRNA. Second, k_{obs} for the two-piece tRNA were measured at a single NTP concentration (1 mM), which does not take into account differences in NTP binding affinity (K_D) for each base-pairing combination (Nakamura et al. 2018b). In several cases, k_{obs} may not yet have reached its maximal values due to the fact that 1 mM NTP is not sufficient to have achieved

saturation for many combinations of NTP and RNA where K_D values are in the $>100 \mu\text{M}$ range. We emphasize that a different Thg1 enzyme (*C. albicans* Thg1) was used in the two-piece assays. However, faster rates with full-length tRNA vs. two-piece substrates (by ~ 15 -fold) were also reported even with this enzyme (Nakamura et al. 2018b), suggesting that the observed differences cannot be entirely explained by the different sources of enzyme used in these studies. Thus, although the two-piece tRNA systems have some significant technical advantages and have been used for interesting applications (Desai et al. 2018; Nakamura et al. 2018b), there are also some challenges for fully assessing the kinetics of 3'-5' addition that should be considered, particularly for reactions that occur with lower efficiency than the G_{-1} incorporation or WC base-paired reactions.

For the physiological A_{73} -tRNA^{His} substrate, a comparison of the relative k_{pol}/K_D values measured here suggests that UTP would be the most frequently misincorporated NTP by SceThg1, occurring $\sim 4.5\%$ of the time compared to GTP, followed by ATP 0.4% of the time, and CTP with an even lower frequency of 0.03% (Table 1). Interestingly, this pattern matches the observed frequency of nucleotide incorporations at the -1 position of tRNA^{His} in vivo in wild-type *S. cerevisiae* almost exactly (Dodbele et al. 2019). In this case, U_{-1} was detected at 4.1% of all tRNA that contain a -1 nucleotide (81% of the total tRNA^{His} pool), with the amount of A_{-1} correspondingly lower (1.6%) and the level of C_{-1} estimated at $<1\%$ based on RNA-seq data. Thus, the differences observed here under our conditions, where even low-efficiency rates of forming other non-WC base pairs could be assessed, appear to be consistent with the overall biological preferences of SceThg1.

Base-pair selection by SceThg1 is driven by the rate of nucleotidyl transfer

Because we were able to measure both maximal rates (k_{pol}) and apparent affinity (K_D) for each NTP: N_{73} combination, we were able to compare how each of these features contribute to base-pair selection by SceThg1. The apparent affinity of SceThg1 for each NTP substrate (K_D) varied substantially for different base-pair combinations, and also depends on the identity of the template nucleotide in the substrate RNA (Table 1). Generally, purine NTPs are bound more tightly than pyrimidines during nucleotidyl transfer by about two- to 50-fold, with GTP binding most tightly to all substrates tested, consistent with its generally high catalytic efficiency (Table 1). Very tight binding of GTP to C_{73} -RNA was evident from the inability to achieve subsaturating concentrations of GTP in any assays. We observed no change in k_{obs} from the maximal value reported in Table 1, even at concentrations as low as $1 \mu\text{M}$ GTP. Therefore, K_D is reported as an upper limit for the GTP: C_{73} combination, and the affinity for GTP in the context

of its WC base-paired template is greater than any other NTP by at least 100-fold (Table 1). However, for all non-WC GTP:template combinations (tRNAs with A_{73} , G_{73} , or U_{73}), the difference between affinity for GTP vs. ATP was only two- to threefold. Moreover, patterns of affinity for other non-WC combinations follow inconsistent trends, with at least one non-WC combination (ATP: A_{73}) binding even tighter than the WC base-paired UTP: A_{73} combination. Thus, contributions from NTP binding affinity are not the primary determinant of SceThg1's base-pair selection efficiency.

In contrast to the relatively modest differences in K_D that do not strictly correlate with WC base-pair forming potential, the correct WC base-pairing NTP was always incorporated with a maximal rate (k_{pol}) that is the next highest after the k_{pol} for GTP (Table 1). Moreover, k_{pol} values for either GTP or a WC base-pairing NTP are greater than k_{pol} for any other non-WC NTP for any substrate tested. Thus, the higher catalytic efficiencies for incorporating GTP, and secondarily for WC base-pairing NTPs, are driven more substantially by the enhanced catalytic rate for these substrate combinations. Interestingly, GTP in the context of the G:C WC base pair seems to benefit from both GTP and WC preference, and thus represents a special case where both faster rates and higher apparent affinity appear to drive the overwhelming ($>10^4$ -fold) preference of SceThg1 for this nucleotide addition reaction (Table 1).

The Hoogsteen face of GTP plays a role in base-pair recognition in the context of full-length tRNA^{His}

Previously the two-piece tRNA system had been used to study behavior of *C. albicans* Thg1 with various GTP analogs, revealing that only nucleotides in the syn conformation are competent for catalysis, and an extremely efficient addition of ITP in the context of A_{73} , but not other template nucleotides (Nakamura et al. 2018b). Given the kinetic differences observed here when using full-length substrates, some of these patterns with GTP analogs were revisited here with SceThg1 (Fig. 3A). Single-turnover reactions were performed with 1 mM of the indicated GTP analog, which is the same NTP concentration tested with the two-piece substrates. Since complete kinetic profiles were not obtained for each analog, measured rates are reported as k_{obs} values (Table 2). Three template tRNA were used to test the physiological non-WC (G_{-1} : A_{73}), WC (G_{-1} : C_{73}) and non-WC (G_{-1} : G_{73}) addition reactions with each analog. Interestingly, all three tRNA substrates showed generally similar patterns of activity with the 7-deaza-GTP and 8-oxo-GTP incorporations, with addition occurring at much slower rates between 1%–3% of the rate for GTP incorporation into the same substrate (Table 2; Fig. 3B). This is in contrast to the stark difference in behavior of these two analogs in the two-piece assay, where the

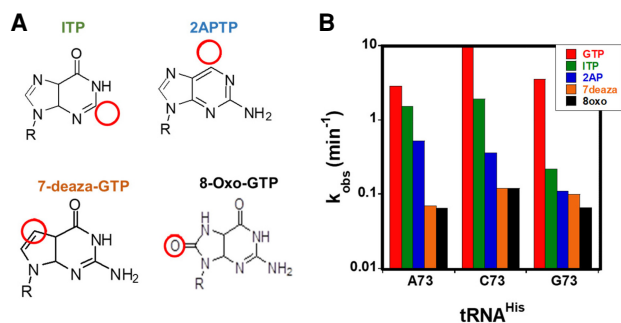


FIGURE 3. Single-turnover measurement of nucleotidyl transfer with GTP analogs and full-length 5'ppp-tRNA^{His} substrates. (A) Chemical structures of selected analogs tested in nucleotidyl transfer reactions. Differences from standard GTP nucleotides are highlighted with red circles on each diagram; R indicates ribose 5'-triphosphate. (B) Single-turnover rate (k_{obs}) of nucleotidyl transfer was measured using the 5'-ppp-tRNA^{His} substrate (as indicated) in the presence of 1 mM of each GTP analog [GTP (red), ITP (green), 2APTP (blue), 7-deaza-GTP (orange) and 8-oxo-GTP (black)] and 15 μ M SceThg1.

7-deaza analog was relatively better tolerated (\sim 4%–15% of k_{obs} for GTP), and the 8-oxo analog substantially less well-tolerated (no detectable activity with any tested substrate). This difference may also reflect distinct preferences of the two enzymes used in these assays (SceThg1 vs. *C. albicans* Thg1). Interestingly, the identity of the tRNA N₇₃ template had relatively little effect on activity with either of these analogs with changes at N7 or C8 positions. However, a stronger template-dependence was observed for the ITP and 2APTP addition reactions, which is similar to the results observed for the two-piece tRNA for these analogs (Nakamura et al. 2018b). For ITP, rates of addition to the A₇₃ and C₇₃ tRNA was within two- to fivefold of the GTP k_{obs} value, while there was a more substantial (16-fold) effect on incorporation of ITP with the G₇₃-tRNA. A similar N₇₃-dependent trend was observed with 2APTP. We did not observe a strong stimulation of the rate of incorporation with ITP and the full-length A₇₃-tRNA, in contrast to what was observed with the analogous two-piece substrate, where the rate was \sim 300% of that with a standard GTP. This intriguing substrate-dependent difference is yet to be explained and will likely require future structural characterization to fully rationalize.

Identification of SceThg1 residues that participate in non-WC (G₋₁-A₇₃tRNA^{His}) base-pair recognition

Thg1-type and TLP-type members of the Thg1 superfamily exhibit distinct preferences for WC versus non-WC base-pair formation. Specifically, while Thg1 enzymes efficiently form the G₋₁:A₇₃ tRNA^{His} base pair as part of their biological reaction, TLPs do not perform this non-WC reaction efficiently (Abad et al. 2010; Rao et al. 2011). Thus, we hypothesized that a comparison of Thg1 and TLP enzyme sequences might reveal conserved residues that correlate with each family member's biochemical properties, including base-pair recognition. Sequence alignments were used to identify residues that were highly conserved among Thg1-type enzymes, and which were not conserved similarly among TLPs. Using this approach, we identified three positions that met these criteria, which correspond to residues N46, Y160 and T185 in SceThg1 (Fig. 4A). Variants were constructed to replace the Thg1-specific residue in SceThg1 to another residue depending on features of the local alignment, yielding N46Y, Y160M, and T185A SceThg1. Although the alignment suggested smaller replacements for Y160 might recapitulate features of the TLP, comparison with the structure of BtTLP indicated a downstream methionine occupies an analogous position (Hyde et al. 2013), leading us to create the Y160M variant that turned out to be successful in the experiment described below.

Recently, alterations of several conserved Thg1 residues in the context of human Thg1 revealed that residues that affect base-pair recognition exert a stronger kinetic effect on the first (adenylation) step of the Thg1 reaction with tRNA^{His} than on the second (nucleotidyl transfer) step (Matlock et al. 2019). Therefore, observed rates were measured for each purified SceThg1 variant under single-turnover conditions using 5'-monophosphorylated tRNA^{His} (p-tRNA). Consistent with previous results, the k_{obs} for both non-WC (G₋₁:A₇₃) and WC (G₋₁:C₇₃) reactions catalyzed by wild-type SceThg1 with p-tRNA differ by only approximately twofold, with a slight preference for the WC reaction (Table 3; Fig. 4B). The lower k_{obs} values measured for WT SceThg1 with p-tRNA compared with ppp-tRNA also agree with previous kinetic measurements, which

TABLE 2. GTP analog incorporation by SceThg1 into tRNA^{His} variant substrates

tRNA ^{His}	k_{obs} (min ⁻¹)				
	GTP ^a	ITP	2APTP	7-Deaza-GTP	8-Oxo-GTP
A ₇₃	2.84 ± 0.08	1.55 ± 0.03	0.57 ± 0.06	0.067 ± 0.002	0.066 ± 0.002
C ₇₃	≥10	1.90 ± 0.16	0.36 ± 0.03	0.12 ± 0.01	0.12 ± 0.01
G ₇₃	3.56 ± 0.39	0.22 ± 0.02	0.11 ± 0.01	0.100 ± 0.009	0.066 ± 0.002

^a k_{obs} value is extrapolated from k_{pol} values measured for GTP in Table 1. Based on measured K_D values, k_{obs} at 1 mM GTP should correspond to k_{pol} for each tRNA substrate.

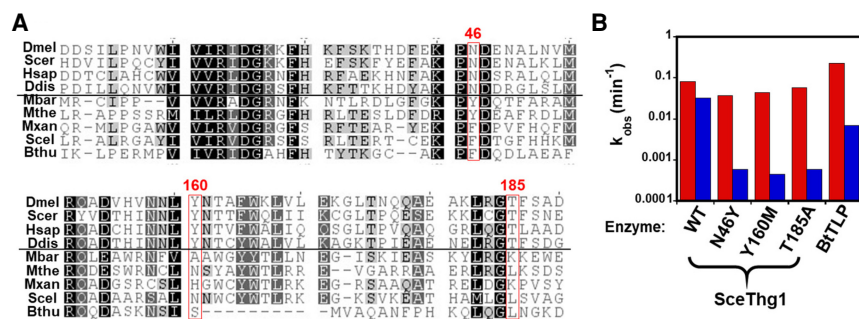


FIGURE 4. Identification of SceThg1 residues that affect non-WC base-paired nucleotide addition. (A) Selected segments from a multiple sequence alignment of Thg1 enzymes from *D. melanogaster* (Dmel), *S. cerevisiae* (Scer), *H. sapiens* (Hsap), and *D. discoideum* (Ddis) compared with TLP enzymes from *M. barkeri* (Mbar), *M. thermoautotrophicus* (Mthe), *M. xanthus* (Mxan), *S. celluloseus* (Scel), and *B. thuringiensis* (Bthu). The top panel shows a region corresponding to residues 15–54 of SceThg1; the bottom panel shows a region corresponding to residues 150–189 of SceThg1. Residues altered in SceThg1 in this work are highlighted in red. (B) G_{-1} addition activities of purified SceThg1 WT and variants (15 μ M each) measured under single-turnover conditions with 5^{32} P-labeled monophosphorylated $tRNA^{His}$ substrates. Red bars correspond to measured k_{obs} for addition of WC base-paired G_{-1} to C_{73} - $tRNA^{His}$, and blue bars correspond to k_{obs} for addition of non-WC base-paired G_{-1} to A_{73} - $tRNA^{His}$. Control reactions with BtTLP were performed under identical conditions to indicate the expected TLP preference for WC over non-WC base-pair formation.

revealed that the slower adenylation step is rate limiting under these conditions (pH 7.5) (Smith and Jackman 2012). Control reactions with a bacterial TLP from *Bacillus thuringiensis* (BtTLP) also demonstrate the expected preference for WC G_{-1} : C_{73} addition by a TLP, with \sim 30-fold higher k_{obs} for this reaction than for G_{-1} : A_{73} (Table 3; Fig. 4B). Interestingly, the single residue SceThg1 variants all exhibited a substantial (50–100-fold) defect in the k_{obs} for the non-WC addition of GTP to A_{73} - $tRNA^{His}$, while exhibiting virtually no effect on the rate of the WC addition of GTP to C_{73} - $tRNA^{His}$ (Table 3; Fig. 4B). Thus, these three conserved residues (N46, Y160 and T185) appear to be required for some interaction that enables SceThg1 to form the non-WC G_{-1} : A_{73} base pair, but which is not required for formation of the WC G_{-1} : C_{73} base pair. The lack of conservation of these residues among TLPs appears to reflect the fact that forming the G_{-1} : A_{73} base pair is not these

enzymes' physiological role. In the converse experiment, we tested whether replacement of the BtTLP residues at these positions with the SceThg1-type N46, Y160 and T185 would result in increased ability of the resulting variant to add the non-WC GTP to the A_{73} - $tRNA$, but saw no detectable increase in non-WC activity with any of the tested enzymes (data not shown). These data suggest that acquisition of the ability to form the non-WC G_{-1} : A_{73} base pair is more complicated in the context of an enzyme that has not evolved to catalyze this activity.

DISCUSSION

Previous studies have shown that Thg1 family enzymes share significant structural similarity with canonical DNA polymerases including the positioning of two metal ions that are critical for catalysis (Hyde et al. 2010, 2013; Nakamura et al. 2013; Kimura et al. 2016). For the first time, we have shown using single-turnover kinetic assays that the Thg1 family of polymerases also share similar aspects of their kinetic mechanism with many 5'-3' polymerases. Similar to several well-studied canonical polymerases, nucleotide incorporation is driven mainly by faster rate constants (k_{po}) for certain base-pairing combinations, rather than by significant effects on the dissociation constant (K_D) for certain NTP:RNA combinations. Our kinetic analyses predict the existence of two biochemically distinct components of the SceThg1 active site, one for mediating non-WC GTP addition and the second for WC base-pair formation.

We show that the ability to add a non-WC GTP base pair, the hallmark of eukaryotic Thg1-type activity, is driven by a unique kinetic preference for GTP as the nucleotide donor

TABLE 3. Single-turnover rate (k_{obs}) for G_{-1} addition catalyzed by SceThg1 variants^a

Enzyme	k_{obs} (min^{-1}) A_{73} - $tRNA^{His}$	k_{obs} (min^{-1}) C_{73} - $tRNA^{His}$	Fold-difference (WC/non-WC) ^c
WT	0.033 ± 0.002	0.08 ± 0.06	2
N46Y	0.00059^b	0.0360 ± 0.0006	60
Y160M	0.00046^b	0.044 ± 0.009	96
T185A	0.00059^b	0.058 ± 0.007	98
BtTLP	0.007 ± 0.001	0.23 ± 0.08	33

^aSingle turnover k_{obs} were measured in reactions with 0.1 mM ATP and 1 mM GTP and the indicated $tRNA^{His}$ substrate with saturating concentration of purified SceThg1 or BtTLP enzymes.

^b k_{obs} was determined using method of linear initial rates.

^cFold difference calculated as $k_{obs}(C_{73}\text{-}tRNA^{His})/k_{obs}(A_{73}\text{-}tRNA^{His})$.

for 3′–5′ addition. In addition, we find that the catalytic efficiency (k_{pol}/K_D) of GTP incorporation is approximately five- to 22-fold higher compared to any other WC base-pair addition across all N_{73} tRNA^{His} substrates. These observations are consistent with the biological requirement for SceThg1 to add G_{-1} to tRNA^{His}, but also reveal that the physiological non-WC $G_{-1}:A_{73}$ reaction is not strictly “templated” because it occurs with nearly identical catalytic efficiency as $G_{-1}:G_{73}$ and $G_{-1}:U_{73}$ reactions (Table 1).

Using transient kinetic assays, we also showed that the WC base substitution fidelity of SceThg1 varies substantially, ranging from 10^{-1} to 10^{-6} for nucleotide incorporation across from various N_{73} -tRNA^{His}. This contrasts with the canonical high-fidelity polymerases which display a fidelity range of 10^{-6} to 10^{-8} (Kuchta et al. 1988), and instead is more appropriately compared to Y-Family DNA polymerase enzymes, which play roles in DNA repair (McCulloch and Kunkel 2008). We note that the relatively slow rates for Thg1 catalysis (in the min^{-1} range), compared to many high-fidelity polymerases that operate in the 10^2 sec^{-1} regime, also suggests that 3′–5′ polymerases are more aptly compared to repair polymerases that typically exhibit slower catalytic rates of NTP incorporation. Fidelity exhibited by canonical polymerases is only partly explained by free energy differences between WC and non-WC base-pairing (Petruska et al. 1988). In addition, substrate induced conformational changes, a tight complementary fit between the nascent base pair and the nascent base-pair-binding pocket, and 3′–5′ exonucleolytic proofreading activity of the polymerase all significantly enhance the level of base selectivity and incorporation efficiency (Beard et al. 2002; Kool 2002). The difference in fidelity between many DNA polymerases and Thg1 polymerases can partly be accounted for by the fact that Thg1 polymerases use little to no difference in ground state binding affinity K_D to discriminate between most WC and non-WC base-pair additions (Table 1), while high-fidelity polymerases can discriminate up to three orders of magnitude (Johnson 2010). Similar to low-fidelity DNA polymerases, Thg1 family polymerases may also exhibit a relatively more open and solvent accessible active site for N_{-1} addition that enables more flexibility in accommodating a nascent incoming base pair (Ling et al. 2001; Trincao et al. 2001; Wong et al. 2008). It is also apparent that mismatched purines bind ~three- to 30-fold better than mismatched pyrimidines. This preference for stronger purine binding might be explained by the presence of base stacking interactions with the incoming NTP in the Thg1 active site, which have also been observed in the structure of a TLP with bound NTP in the repair conformation (Friedman and Honig 1995; Kimura et al. 2016).

Kinetic measurements using different GTP nucleotide analogs showed that the atoms on the Hoogsteen face of the incoming GTP may be involved in positioning the nucleotide for nucleotidyl transfer regardless of the templating

N_{73} base. Thus, at least some features of the active site that interact with this Hoogsteen face of the incoming NTP might be shared for both WC and non-WC reactions. Although not identical in terms of the magnitude of defects, some similarities with effects of GTP analogs on activity of *C. albicans* Thg1 suggest that this feature is conserved among Thg1-type enzymes. These enzymes, which are capable of efficiently forming both WC and non-WC base-pairs with GTP, may have an asymmetric active site similar to that exhibited by DNA polymerase *iota*, which allows distinct base-pairing modes depending upon the nature of the templating base (Choi et al. 2009). Our observation of amino acids that are preferentially required for efficient incorporation of GTP in the non-WC base-paired context (Fig. 4) suggests that at least some of these features can be separated biochemically. This idea is consistent with recent observations, where highly conserved residues H152 and K187 in human Thg1 also are uniquely required for the non-WC $G_{-1}:A_{73}$ reaction, and are not critical for WC base-paired $G_{-1}:C_{73}$ or $U_{-1}:A_{73}$ reactions (Matlock et al. 2019).

There are currently two available crystal structures of Thg1-type members of the 3′–5′ polymerase family from eukaryotic sources (*human* and *C. albicans*) (Hyde et al. 2010; Nakamura et al. 2013). However, none of the conserved amino acid residues (N46, Y160, T185) identified to affect non-WC GTP incorporation here are observed to make specific contacts with NTP or tRNA in the Thg1 active site in either of these structures. Thus, the molecular basis for this remains to be fully determined. It is possible that conformational changes following formation of the ternary complex (Thg1:NTP:tRNA) could occur during the course of the reaction similar to what has been proposed for several canonical polymerases. Further experiments will be needed to fully understand the molecular role of these conserved residues, and to comprehensively identify the components of the Thg1 active site that participate in each type of base-pairing reaction.

MATERIALS AND METHODS

Thg1–TLP protein expression and purification

SceThg1 (Gu et al. 2003) and BtTLP (Rao et al. 2011) genes cloned into pET expression vectors containing N-terminal His₆-tag were transformed into *E. coli* BL21(DE3) pLysS. Overexpressed amino-terminal His₆-tagged protein was purified using immobilized metal-ion affinity chromatography (IMAC), as previously described (Smith and Jackman 2012). Purified proteins were judged to be >90% pure by SDS–PAGE and stored at -20°C , while the BioRad protein assay was used to determine the concentrations of purified proteins for subsequent activity assays.

In vitro transcription of tRNA constructs

T7 RNA polymerase was used for runoff in vitro transcription using digested plasmids encoding tRNA^{His} variant constructs

downstream from the T7 RNA polymerase promoter, as previously described (Rao et al. 2011). The tRNA^{His} variant constructs were transcribed in the presence of [γ -³²P] GTP (6000 Ci/mmol, Perkin-Elmer) to obtain [γ -³²P]ppp-labeled tRNA^{His} (5'-*ppp-tRNA), according to published methods (Jackman and Phizicky 2006b).

Single-turnover nucleotidyl transfer assays

To determine kinetic parameters for the nucleotidyl transfer step, 5'-*ppp-tRNA^{His} substrates (100–300 nM) generated using in vitro transcription were reacted with NTP in Thg1 reaction buffer (25 mM HEPES pH 7.5, 10 mM MgCl₂, 125 mM NaCl, 3 mM DTT, 0.2 mg/mL bovine serum albumin [BSA]) at room temperature as described previously (Smith and Jackman 2012). The concentration of SceThg1 used in the assays (15 μ M) was previously determined to be saturating for G₋₁ addition activity under these conditions (Smith and Jackman 2012). In addition to standard NTPs, various GTP analogs (Trilink Biotechnologies) including inosine triphosphate (ITP), 2-aminopurine triphosphate (2AATP), 7-deazaguanosine triphosphate (7-deaza-GTP) and 8-oxoguanosine triphosphate (8-oxo-GTP) were also used to measure k_{obs} for nucleotide addition to the indicated *ppp-tRNA^{His}. To quench reactions, 3 μ L aliquots were taken out of the reaction mixture at various time points and added to a new tube containing 1 μ L of 500 mM EDTA. Following this step, 2 μ L of each quenched reaction mixture was spotted on to PEI-cellulose TLC plates (EM Science). To separate the labeled pyrophosphate (PP_i) product released after NTP addition from unreacted labeled tRNA substrate, the TLC plates were washed in 100% methanol, air-dried, and resolved using a 0.5 M potassium phosphate (pH 6.3)/methanol (80:20) solvent system. Time courses of product formation were plotted and fit to a single-exponential rate equation (Equation 1) using Kaleidagraph (Synergy Software).

$$P_t = \Delta P[1 - \exp(-k_{obs}t)], \quad (1)$$

where P_t is the fraction of product formed at each time and ΔP is the maximal amount of product conversion observed during each time course.

The pseudo-first order maximal rate constants k_{pol} and apparent dissociation constants (K_D) were determined by plotting the resulting k_{obs} values determined for each [NTP] and fitting the data to Equation 2. The reported kinetic parameters were determined from data derived from at least three independent assays for each tRNA/NTP combination.

$$k_{obs} = k_{pol}*[NTP]/(K_{D,app-NTP} + [NTP]). \quad (2)$$

Preparation of SceThg1 variants

SceThg1 variants N46Y, Y160M and T185A were constructed using the Phusion mutagenesis protocol according to the manufacturer's instructions, using complementary pairs of oligonucleotides and validated by DNA sequencing. The plasmid encoding amino-terminal His₆-tagged SceThg1 was used as the template for the mutagenesis experiment. Thg1 variant proteins were purified using immobilized metal ion affinity chromatography (IMAC) as described above for the wild-type enzyme.

G₋₁ nucleotide addition to 5'-monophosphorylated tRNA with SceThg1 variants

G₋₁ addition reactions were performed at room temperature by reacting 5'-monophosphorylated [³²P]-tRNA^{His} (5'-p*tRNA^{His}) substrate (≤ 40 nM) with 0.1 mM ATP and 1 mM GTP in the presence of excess enzyme (15 μ M). The 5'-p*tRNA^{His} (with A₇₃ or C₇₃) was generated by in vitro transcription followed by calf intestinal phosphatase (NEB) treatment and labeling with T4 polynucleotide kinase (NEB), as previously described (Jackman and Phizicky 2006a). To measure the k_{obs} , a saturating amount of enzyme (15 μ M SceThg1) was added to a reaction mixture containing p*tRNA^{His}, 0.1 mM ATP, 1 mM GTP in Thg1 reaction buffer. At specific time points, a 3 μ L aliquot was removed from the reaction mixture and quenched by adding 1 mg/mL of RNaseA (Ambion) and 500 mM EDTA. The quenched reaction mixture was incubated at 50°C for 10 min. RNaseA digested samples were treated with 0.5 U calf intestinal phosphatase (CIP) (Invitrogen) and incubated at 37°C for 30 min. The products were resolved and quantified using silica thin-layer chromatography (TLC), as described previously (Jackman and Phizicky 2006a; Rao et al. 2011; Smith and Jackman 2012).

ACKNOWLEDGMENTS

Funding for this work was provided by the National Institutes of Health (NIH) R01 GM087543 and S10 OD023582 to J.E.J.

Received January 22, 2021; accepted March 23, 2021.

REFERENCES

- Abad MG, Rao BS, Jackman JE. 2010. Template-dependent 3'-5' nucleotide addition is a shared feature of tRNA^{His} guanylyltransferase enzymes from multiple domains of life. *Proc Natl Acad Sci* **107**: 674–679. doi:10.1073/pnas.0910961107
- Abad MG, Long Y, Willcox A, Gott JM, Gray MW, Jackman JE. 2011. A role for tRNA^{His} guanylyltransferase (Thg1)-like proteins from *Dictyostelium discoideum* in mitochondrial 5'-tRNA editing. *RNA* **17**: 613–623. doi:10.1261/ma.2517111
- Abad MG, Long Y, Kinchen RD, Schindel ET, Gray MW, Jackman JE. 2014. Mitochondrial tRNA 5'-editing in *Dictyostelium discoideum* and *Polysphondylium pallidum*. *J Biol Chem* **289**: 15155–15165. doi:10.1074/jbc.M114.561514
- Beard WA, Shock DD, Vande Berg BJ, Wilson SH. 2002. Efficiency of correct nucleotide insertion governs DNA polymerase fidelity. *J Biol Chem* **277**: 47393–47398. doi:10.1074/jbc.M210036200
- Brown JA, Zhang L, Sherrer SM, Taylor JS, Burgers PM, Suo Z. 2010. Pre-steady-state kinetic analysis of truncated and full-length *Saccharomyces cerevisiae* DNA polymerase ϵ . *J Nucleic Acids* **2010**: 871939. doi: 10.4061/2010/871939
- Chen G, Kennedy SD, Qiao J, Krugh TR, Turner DH. 2006. An alternating sheared AA pair and elements of stability for a single sheared purine-purine pair flanked by sheared GA pairs in RNA. *Biochemistry* **45**: 6889–6903. doi:10.1021/bi0524464
- Chen AW, Jayasinghe MI, Chung CZ, Rao BS, Kenana R, Heinemann IU, Jackman JE. 2019. The role of 3' to 5' reverse RNA polymerization in tRNA fidelity and repair. *Genes (Basel)* **10**: 250. doi:10.3390/genes10030250
- Choi JY, Lim S, Eoff RL, Guengerich FP. 2009. Kinetic analysis of base-pairing preference for nucleotide incorporation opposite template

- pyrimidines by human DNA polymerase ϵ . *J Mol Biol* **389**: 264–274. doi:10.1016/j.jmb.2009.04.023
- Desai R, Kim K, Buchsenschutz HC, Chen AW, Bi Y, Mann MR, Turk MA, Chung CZ, Heinemann IU. 2018. Minimal requirements for reverse polymerization and tRNA repair by tRNA^{His} guanylyltransferase. *RNA Biol* **15**: 614–622. doi:10.1080/15476286.2017.1372076
- Dodbele S, Moreland B, Gardner SM, Bundschuh R, Jackman JE. 2019. 5'-end sequencing in *Saccharomyces cerevisiae* offers new insights into 5'-ends of tRNA^{His} and snoRNAs. *FEBS Lett* **593**: 971–981. doi:10.1002/1873-3468.13364
- Fiala KA, Suo Z. 2004. Pre-steady-state kinetic studies of the fidelity of *Sulfolobus solfataricus* P2 DNA polymerase IV. *Biochemistry* **43**: 2106–2115. doi:10.1021/bi0357457
- Friedman RA, Honig B. 1995. A free energy analysis of nucleic acid base stacking in aqueous solution. *Biophys J* **69**: 1528–1535. doi:10.1016/S0006-3495(95)80023-8
- Gu W, Jackman JE, Lohan AJ, Gray MW, Phizicky EM. 2003. tRNA^{His} maturation: an essential yeast protein catalyzes addition of a guanine nucleotide to the 5' end of tRNA^{His}. *Genes Dev* **17**: 2889–2901. doi:10.1101/gad.1148603
- Gu W, Hurto RL, Hopper AK, Grayhack EJ, Phizicky EM. 2005. Depletion of *Saccharomyces cerevisiae* tRNA^{His} guanylyltransferase Thg1p leads to uncharged tRNA^{His} with additional m⁵C. *Mol Cell Biol* **25**: 8191–8201. doi:10.1128/MCB.25.18.8191-8201.2005
- Hyde SJ, Eckenroth BE, Smith BA, Eberley WA, Heintz NH, Jackman JE, Double S. 2010. tRNA^{His} guanylyltransferase (THG1), a unique 3'–5' nucleotidyl transferase, shares unexpected structural homology with canonical 5'–3' DNA polymerases. *Proc Natl Acad Sci* **107**: 20305–20310. doi:10.1073/pnas.1010436107
- Hyde SJ, Rao BS, Eckenroth BE, Jackman JE, Double S. 2013. Structural studies of a bacterial tRNA^{His} guanylyltransferase (Thg1)-like protein, with nucleotide in the activation and nucleotidyl transfer sites. *PLoS One* **8**: e67465. doi:10.1371/journal.pone.0067465
- Jackman JE, Phizicky EM. 2006a. tRNA^{His} guanylyltransferase adds G₋₁ to the 5' end of tRNA^{His} by recognition of the anticodon, one of several features unexpectedly shared with tRNA synthetases. *RNA* **12**: 1007–1014. doi:10.1261/ma.54706
- Jackman JE, Phizicky EM. 2006b. tRNA^{His} guanylyltransferase catalyzes a 3'–5' polymerization reaction that is distinct from G₋₁ addition. *Proc Natl Acad Sci* **103**: 8640–8645. doi:10.1073/pnas.0603068103
- Jackman JE, Gott JM, Gray MW. 2012. Doing it in reverse: 3'-to-5' polymerization by the Thg1 superfamily. *RNA* **18**: 886–899. doi:10.1261/ma.032300.112
- Jahn D, Pande S. 1991. Histidine tRNA guanylyltransferase from *Saccharomyces cerevisiae*. II. Catalytic mechanism. *J Biol Chem* **266**: 22832–22836. doi:10.1016/S0021-9258(18)54429-X
- Johnson KA. 2010. The kinetic and chemical mechanism of high-fidelity DNA polymerases. *Biochim Biophys Acta* **1804**: 1041–1048. doi:10.1016/j.bbapap.2010.01.006
- Johnson AA, Johnson KA. 2001. Fidelity of nucleotide incorporation by human mitochondrial DNA polymerase. *J Biol Chem* **276**: 38090–38096. doi:10.1074/jbc.M106045200
- Joyce CM, Benkovic SJ. 2004. DNA polymerase fidelity: kinetics, structure, and checkpoints. *Biochemistry* **43**: 14317–14324. doi:10.1021/bi048422z
- Joyce CM, Steitz TA. 1995. Polymerase structures and function: variations on a theme? *J Bacteriol* **177**: 6321–6329. doi:10.1128/JB.177.22.6321-6329.1995
- Kimura S, Suzuki T, Chen M, Kato K, Yu J, Nakamura A, Tanaka I, Yao M. 2016. Template-dependent nucleotide addition in the reverse (3'–5') direction by Thg1-like protein. *Sci Adv* **2**: e1501397. doi:10.1126/sciadv.1501397
- Kool ET. 2002. Active site tightness and substrate fit in DNA replication. *Annu Rev Biochem* **71**: 191–219. doi:10.1146/annurev.biochem.71.110601.135453
- Kuchta RD, Benkovic P, Benkovic SJ. 1988. Kinetic mechanism whereby DNA polymerase I (Klenow) replicates DNA with high fidelity. *Biochemistry* **27**: 6716–6725. doi:10.1021/bi00418a012
- Ling H, Boudsocq F, Woodgate R, Yang W. 2001. Crystal structure of a Y-family DNA polymerase in action: a mechanism for error-prone and lesion-bypass replication. *Cell* **107**: 91–102. doi:10.1016/S0092-8674(01)00515-3
- Long Y, Abad MG, Olson ED, Carrillo EY, Jackman JE. 2016. Identification of distinct biological functions for four 3'–5' RNA polymerases. *Nucleic Acids Res* **44**: 8395–8406. doi:10.1093/nar/gkw681
- Matlock AO, Smith BA, Jackman JE. 2019. Chemical footprinting and kinetic assays reveal dual functions for highly conserved eukaryotic tRNA^{His} guanylyltransferase residues. *J Biol Chem* **294**: 8885–8893. doi:10.1074/jbc.RA119.007939
- McCulloch SD, Kunkel TA. 2008. The fidelity of DNA synthesis by eukaryotic replicative and translesion synthesis polymerases. *Cell Res* **18**: 148–161. doi:10.1038/cr.2008.4
- Nakamura A, Nemoto T, Heinemann IU, Yamashita K, Sonoda T, Komoda K, Tanaka I, Soll D, Yao M. 2013. Structural basis of reverse nucleotide polymerization. *Proc Natl Acad Sci* **110**: 20970–20975. doi:10.1073/pnas.1321312111
- Nakamura A, Wang D, Komatsu Y. 2018a. Biochemical analysis of human tRNA^{His} guanylyltransferase in mitochondrial tRNA^{His} maturation. *Biochem Biophys Res Commun* **503**: 2015–2021. doi:10.1016/j.bbrc.2018.07.150
- Nakamura A, Wang D, Komatsu Y. 2018b. Molecular mechanism of substrate recognition and specificity of tRNA^{His} guanylyltransferase during nucleotide addition in the 3'–5' direction. *RNA* **24**: 1583–1593. doi:10.1261/ma.067330.118
- Nameki N, Asahara H, Shimizu M, Okada N, Himeno H. 1995. Identity elements of *Saccharomyces cerevisiae* tRNA^{His}. *Nucleic Acids Res* **23**: 389–394. doi:10.1093/nar/23.3.389
- Petruska J, Goodman MF, Boosalis MS, Sowers LC, Cheong C, Tinoco I Jr. 1988. Comparison between DNA melting thermodynamics and DNA polymerase fidelity. *Proc Natl Acad Sci* **85**: 6252–6256. doi:10.1073/pnas.85.17.6252
- Rao BS, Maris EL, Jackman JE. 2011. tRNA 5'-end repair activities of tRNA^{His} guanylyltransferase (Thg1)-like proteins from Bacteria and Archaea. *Nucleic Acids Res* **39**: 1833–1842. doi:10.1093/nar/gkq976
- Roettger MP, Fiala KA, Sompalli S, Dong Y, Suo Z. 2004. Pre-steady-state kinetic studies of the fidelity of human DNA polymerase μ . *Biochemistry* **43**: 13827–13838. doi:10.1021/bi048782m
- Rosen AE, Brooks BS, Guth E, Francklyn CS, Musier-Forsyth K. 2006. Evolutionary conservation of a functionally important backbone phosphate group critical for aminoacylation of histidine tRNAs. *RNA* **12**: 1315–1322. doi:10.1261/ma.78606
- Rudinger J, Florentz C, Giege R. 1994. Histidylolation by yeast HisRS of tRNA or tRNA-like structure relies on residues –1 and 73 but is dependent on the RNA context. *Nucleic Acids Res* **22**: 5031–5037. doi:10.1093/nar/22.23.5031
- Rudinger J, Felden B, Florentz C, Giege R. 1997. Strategy for RNA recognition by yeast histidyl-tRNA synthetase. *Bioorg Med Chem* **5**: 1001–1009. doi:10.1016/S0968-0896(97)00061-8
- Smith BA, Jackman JE. 2012. Kinetic analysis of 3'–5' nucleotide addition catalyzed by eukaryotic tRNA^{His} guanylyltransferase. *Biochemistry* **51**: 453–465. doi:10.1021/bi201397f

- Steitz TA. 1998. A mechanism for all polymerases. *Nature* **391**: 231–232. doi:10.1038/34542
- Steitz TA. 1999. DNA polymerases: structural diversity and common mechanisms. *J Biol Chem* **274**: 17395–17398. doi:10.1074/jbc.274.25.17395
- Trincao J, Johnson RE, Escalante CR, Prakash S, Prakash L, Aggarwal AK. 2001. Structure of the catalytic core of *S. cerevisiae* DNA polymerase ϵ : implications for translesion DNA synthesis. *Mol Cell* **8**: 417–426. doi:10.1016/S1097-2765(01)00306-9
- Wong JH, Fiala KA, Suo Z, Ling H. 2008. Snapshots of a Y-family DNA polymerase in replication: substrate-induced conformational transitions and implications for fidelity of Dpo4. *J Mol Biol* **379**: 317–330. doi:10.1016/j.jmb.2008.03.038